Available online at www.sciencedirect.com
ScienceDirect
International Journal of Pharmaceutics 350 (2008) 103–112
INTERNATIONAL JOURNAL OF PHARMACEUTICS
www.elsevier.com/locate/ijpharm

Terpenes increase the partitioning and molecular dynamics of an amphipathic spin label in stratum corneum membranes

Jorge Luiz Vieira dos Anjos, Antonio Alonso *

Instituto de Física, Universidade Federal de Goiás, Goiânia 74001-970, GO, Brazil

Received 24 July 2007; received in revised form 20 August 2007; accepted 20 August 2007
Available online 24 August 2007

Abstract

In this work, the interaction of the skin penetration enhancers DL-menthol, α-terpineol, 1,8-cineole and (+)-limonene with the uppermost skin layer, the stratum corneum and with multilamellar vesicles from 1,2-dipalmitoyl-*sn*-glycero-3-phosphatidylcholine (DPPC) is investigated by electron paramagnetic resonance (EPR) spectroscopy of the small spin label 2,2,6,6,-tetramethylpiperedine-1-oxyl (TEMPO), which partitions the aqueous and hydrocarbon phases. The EPR spectrum allows for the determination of the actual partition coefficient and the rotational diffusion rates of the spin probe in the two environments. The enthalpy changes, ΔH°, to transfer the spin probe from the aqueous to the hydrocarbon phase, as well as the activation energies associated to its rotational motion, were considerably smaller for stratum corneum, indicating less pronounced thermal reorganization. For DPPC, the terpenes increased both the partition coefficient and the rotational diffusion rate of the spin label in the membrane, except in the liquid–crystalline phase, while these increases in stratum corneum were observed in the entire temperature range measured with the exception of the rotational motion parameter for DL-menthol and α-terpineol at temperatures below their melting point (32–41 °C). It is suggested that the terpenes effectively acting as spacers in the membrane fluidize the lipids and cause ruptures in the hydrogen-bonded network of the polar interface.

Keywords: Stratum corneum; EPR; Spin label; Lipid dynamics; Terpene

1. Introduction

The effectiveness of transdermal drug delivery depends on the drug's ability to penetrate the skin sufficiently to reach therapeutic levels. The main skin barrier to exogenous chemical absorption is the outer epidermal layer, the stratum corneum (SC), composed of corneocytes surrounded by a multilamellar lipid matrix. Corneocytes are keratin-filled dead cells containing an insoluble cell envelope of cross-linked proteins, which reduce absorption of drugs into the cells (Bouwstra and Honeywell-Nguyen, 2002), and a cell lipid envelope composed mainly of ω-hydroxyceramides covalently bound to the periphery of the cell envelope (Wertz and Downing, 1987). The intercellular region contains a complex lipid mixture, ordered in multilayered structures known as lipid lamellae and consisting mainly of ceramides, free fatty acids, cholesterol and cholesteryl sulfate.

The most widely implemented approach to overcoming this skin barrier has been the use of chemical penetration enhancers, which ideally alter the physicochemical nature of the SC safely and reversibly to facilitate the drug's delivery through the skin. According to the lipid–protein-partitioning theory (Barry, 1991), penetration enhancers may increase the permeability of a drug by affecting the intercellular lipids of the SC via extraction or fluidization (Yamane et al., 1995), and/or by increasing the partitioning of the drug in the SC membranes (Gao and Singh, 1998), and/or by changing conformations within the keratinized protein component (Williams and Barry, 2004).

Terpenes are naturally occurring compounds derived from essential oils, which contain only carbon, hydrogen and oxygen atoms. Generally used in flavorings, perfumes and medicines, many terpenes including, 1,8-cineole, menthol and α-terpineol, are claimed to be generally recognized as safe (GRAS) materials. Their interactions with the SC are of interest to understand how

Abbreviations: SC, stratum corneum; DPPC, 1,2-dipalmitoyl-*sn*-glycero-3-phosphatidylcholine; TEMPO, 2,2,6,6-tetramethyl-piperidine-1-oxyl; EPR, electron paramagnetic resonance; NLLS, nonlinear least-squares fitting program.

* Corresponding author. Fax: +55 62 3521 1014.
E-mail address: alonso@fis.ufg.br (A. Alonso).

0378-5173/$ – see front matter © 2007 Elsevier B.V. All rights reserved.
doi:10.1016/j.ijpharm.2007.08.024

terpenes, and other small amphiphilic molecules, enhance the permeability of skin. Recently, it was reported that 1,8-cineole and L-menthol applied at 5% (w/v) in solution with 66% ethanol (v/v) provide sufficient zidovudine (AZT) flux in rat skin (more permeable than human skin) to reach its therapeutic concentration (Narishetty and Panchagnula, 2004, 2005). Terpenes have been reported as permeation enhancers of several polar and non-polar drugs such as 5-fluorouracil (Cornwell and Barry, 1994), morphine hydrochloride (Morimoto et al., 2002), propranolol hydrochloride (Hori et al., 1991), imipramine hydrochloride (Jain et al., 2002), indomethacin (Okabe et al., 1989), hydrocortisone (El-Kattan et al., 2000), tamoxifen (Gao and Singh, 1998) and haloperidol (Vaddi et al., 2002a). However, there are only few studies on mechanisms of permeation enhancement by terpenes in SC, which use mainly Fourier-transformed infrared spectroscopy (FTIR), differential scanning calorimetry (DSC) (Vaddi et al., 2002b; Narishetty and Panchagnula, 2004, 2005) and small-angle X-ray diffraction (SAXD) (Cornwell et al., 1996). ATR-FTIR experiments showed that both 1,8-cineole and L-menthol increase CH_2 stretching frequencies and decrease the mid transition temperature (T_m) of a model SC lipid system (Narishetty and Panchagnula, 2005). SAXD experiments showed that D-limonene and 1,8-cineole in propylene glycol decrease the intensity of lipid based reflections, suggesting disruption of lipid packing within the bilayers, while DSC thermograms of these same systems indicated that the terpenes reduce the temperatures of the two major lipid transitions of human SC at 72 and 83 °C (Cornwell et al., 1996).

Spin-labeling electron paramagnetic resonance (EPR) has been employed to obtain information about SC membranes in the intact tissue (Alonso et al., 1995, 1996, 2000; Queirós et al., 2005). It has been shown that hydration of SC increases lipid fluidity (Alonso et al., 1995, 1996), and that the lipid dispersions prepared with extracted SC lipids are much more fluid than the lipids in the intact tissue, whereas the ceramides from the corneocyte lipid envelope, which are covalently bound to the SC proteins, have the lowest state of mobility among the SC lipids (Alonso et al., 2000). The EPR spectra of lipid spin labels in SC membranes are characterized by the coexistence of two spectral components with very different states of mobility. In previous work (Queirós et al., 2005), the origin of these two spectral components was interpreted based on the ability of spin labels to participate in intermolecular hydrogen bonding into the membrane. The more motionally restricted component was assigned to a class of spin probe hydrogen bonded to the polar headgroups (more rigid structure) and the more mobilized component was attributed to those spin labels temporarily nonhydrogen bonded to the polar interface and more deeply inserted in the hydrophobic core. Recently, the effect of the terpenes L-menthol and 1,8-cineole on the SC lipid dynamics was examined in detail (Anjos et al., 2007, 2007a). The presence of 1% terpenes in the solvent drastically increased the lipid fluidity, especially by transferring the spin probes from a more to a less motionally restricted spectral component into the membranes. Furthermore, these two terpenes increased the rotational diffusion rates only of spin probes from the more mobilized component.

The small amphipathic spin label TEMPO partitions between the bilayer and aqueous phase of many membranes (Smirnov et al., 1995). The EPR spectra generally observed for this spin probe in membranes are composed of two spectral components differing in mobility and polarity. The NLLS fitting program allows for the separation of these components, determining their relative fractions and rotational diffusion rates. Since penetration enhancers generally act by favoring drug partition in SC membranes and the spin label TEMPO may mimic drugs, in the present work, we examined the capacity of four terpenes to increase the partitioning and mobility of this spin probe in the SC lipid domain. This small spin probe provides novel findings on the effects of terpenes in SC membranes. Unlike the other spin labels used in previous works (Anjos et al., 2007, 2007a), which are essentially stabilized in the membrane, this spin label allows its partition coefficient between the aqueous and hydrocarbon phases to be monitored. Furthermore, being a small molecule with larger diffusion capacity through the membrane, its rotational motion more accurately reflects the global dynamics of the membrane and its phase transitions. Because the lipid composition of SC is complex, we conducted a parallel study with DPPC membranes to compare the results for SC with those of a simpler and well-known model.

2. Materials and methods

2.1. Preparation of SC membranes

SC membranes of neonatal Wistar rats less than 24 h old were prepared as described previously (Anjos et al., 2007, 2007a). After the animal was killed, its skin was excised and fat was removed by rubbing in distilled water. The skin was allowed to stand for 5 min in a desiccator containing 0.5 L of anhydrous ammonium hydroxide, after which it was floated in distilled water with the internal side in contact with the water for 2 h. The external side was placed in contact with a filter paper and the SC sheet was carefully separated from the remaining epidermis. Subsequently, the SC was transferred to a Teflon-coated screen, washed with distilled water and allowed to dry at room temperature. The membranes were stored with 1 L of silica gel in a desiccator under a moderate vacuum.

2.2. Spin labeling and treatment of SC

To prevent nitroxide reductions, the sulfhydryl groups of the SC tissue were blocked by incubating the SC membranes in a solution of 50 mM *N*-ethyl maleimide (Sigma Chem. Co., St. Louis, MO, USA) for about 15 h. An intact piece of SC (3 mg) was then rinsed with 1.5 mL Milli-Q water and incubated for 90 min at room temperature in 45 μL of acetate-buffered saline (10 mM acetate, 150 mM NaCl and 1 mM EDTA, pH 5.5) containing 0.2 mM spin label TEMPO (Fig. 1) purchased from Sigma Chem. Co., and the corresponding terpene concentration (Acros Organics, Geel, Belgium), which was added to the sample in 5 μL of ethanol. The control samples were subjected in an identical experiment, in which 5 μL of ethanol was added without the terpenes. The intact SC membrane was then intro-

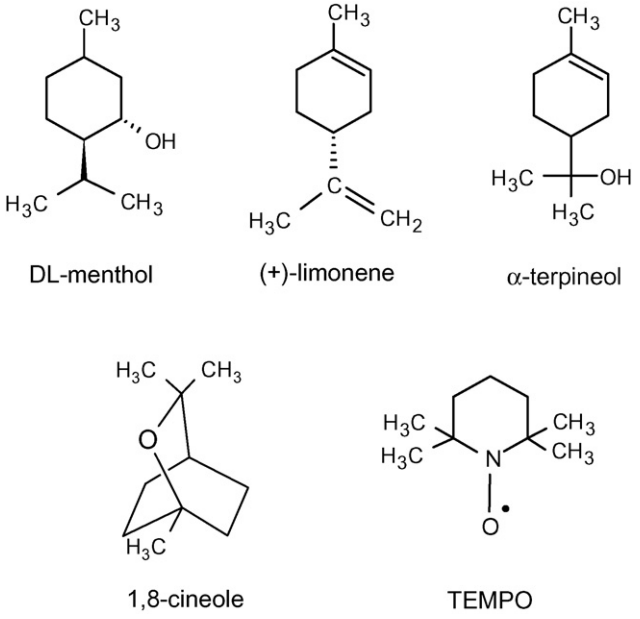

Fig. 1. Chemical structures of spin label TEMPO and terpenes used in this work.

duced into 1 mm i.d. capillary for EPR measurements, the excess solvent was removed and the capillary was flame sealed.

2.3. Preparation of DPPC dispersions

DPPC (3 mg) purchased from Avanti (Alabaster, AL, USA), of >99% purity, was dissolved in 600 μL of a mixture of chloroform:methanol (2:1) and dried under a nitrogen stream. The residual solvent was removed by vacuum-drying the tube overnight. In the hydration step to form multilamellar vesicles of DPPC, the samples were incubated in 0.5 mL of buffer pH 5.5 (the same as that used for SC) for about 5 min at 50 °C and subsequently vortexed several times. The sample volume was reduced to 40 μL by centrifugation at 4 °C and 2 μL of 10 mM TEMPO was added to the DPPC membranes. The calculated concentration of each terpene in ethanol solution (33%, v/v) was added to the sample (about 1.5 μL, depending on the terpene density and no addition was made to the control samples). The DPPC suspension was again vortexed and transferred to a capillary, which was sealed by flame.

2.4. EPR spectroscopy

A Bruker ESP 300 spectrometer equipped with an ER 4102 ST resonator and operating in the X-band (9.4 GHz) was utilized in these investigations. The operating conditions of the equipment were: microwave power of 20 mW; modulation frequency of 100 kHz; modulation amplitude of 0.3 G; magnetic field scan of 100 G; sweep time of 168 s and detector time constant of 41 ms. The temperature was controlled to within 0.3 °C by a nitrogen stream system (Bruker, Rheinstetten, Germany). EPR spectral simulations were performed using the NLLS program developed by Schneider and Freed (1989) and Budil et al. (1996). This program, which allows a single spectrum to be fitted with two components having different mobility and magnetic tensor parameters, gives the relative populations and the associated rotational diffusion rates. Similarly to previous studies (Anjos et al., 2007, 2007a), these parameters were determined based on a general analysis of the overall spectra obtained from this work and, once determined, all the EPR spectra were simulated using the same values. The magnetic parameters used were as follows. Component H: $g_{xx} = 2.0084$, $g_{yy} = 2.0060$, $g_{zz} = 2.0026$; $A_{xx} = 6.5$, $A_{yy} = 6.5$, $A_{zz} = 34.7$ and component P: $g_{xx} = 2.0082$, $g_{yy} = 2.0050$, $g_{zz} = 2.0022$; $A_{xx} = 6.8$, $A_{yy} = 6.8$, $A_{zz} = 38.1$.

3. Results

3.1. Analysis of EPR spectra

The EPR spectra of spin label TEMPO (Fig. 1) in a dispersion of multilamellar vesicles of DPPC or in SC membranes, as well as the measured spectral parameters, are depicted in Fig. 2. Each spectrum is the superposition of the two spectral components H and P, which are provided by the spin label fractions dissolved in the hydrophobic and polar environment, respectively. The parameter f, equal to $H/(H+P)$, was used as the approximate fraction of spin probe dissolved in the membrane (Smirnov et al., 1995). A model of two-spectral components describing an anisotropic Brownian diffusion of TEMPO in both systems was adopted to simulate the EPR spectra and analyze the two superimposed components separately. Fig. 2b shows the same experimental EPR spectrum of Fig. 2a (line), together with its best-fit spectrum (open circles), while Fig. 2c and d show the separate H and P components and their best-fit parameters.

The experimental (line) and best-fit (open circles) EPR spectra of spin label TEMPO in DPPC and SC membranes are shown in Fig. 3 for several temperatures and 1,8-cineole concentrations at 26 °C. As can be noted, the relative population of component H increased gradually as the temperature or terpene concentration increased. Indeed, at 2% terpene in SC (v/v) or at a molecular terpene:DPPC ratio of 2:1 (data not shown), it seems that all the spin probes were displaced to the hydrophobic region.

3.2. Partition coefficient of TEMPO between the hydrocarbon and polar phases

Fig. 4 shows the temperature dependencies of the spectral parameter f and the relative population of component H, N_H, obtained from the fitting. Although the behaviors shown in the plots are similar for these two parameters, there are appreciable discrepancies between the two ways of determining the spin-probe fractions in the bilayers, especially at higher partition coefficients. Both EPR parameters indicated abrupt phase transitions for DPPC at ~34 and ~42 °C, whereas SC membranes were characterized by slight variations, with a higher slope coefficient between ~55 and ~72 °C. For DPPC bilayers, the phase transitions are well known (Shimshick and McConnell, 1973; Wang et al., 1993): the transition at ~34 °C corresponds to the gel structure $L_{\beta'}$ ripple structure $P_{\beta'}$ phase transition, called pre-transition, and the transition at ~42 °C corresponds to a ripple structure $P_{\beta'}$ fluid bilayer structure (Lα) phase transition.

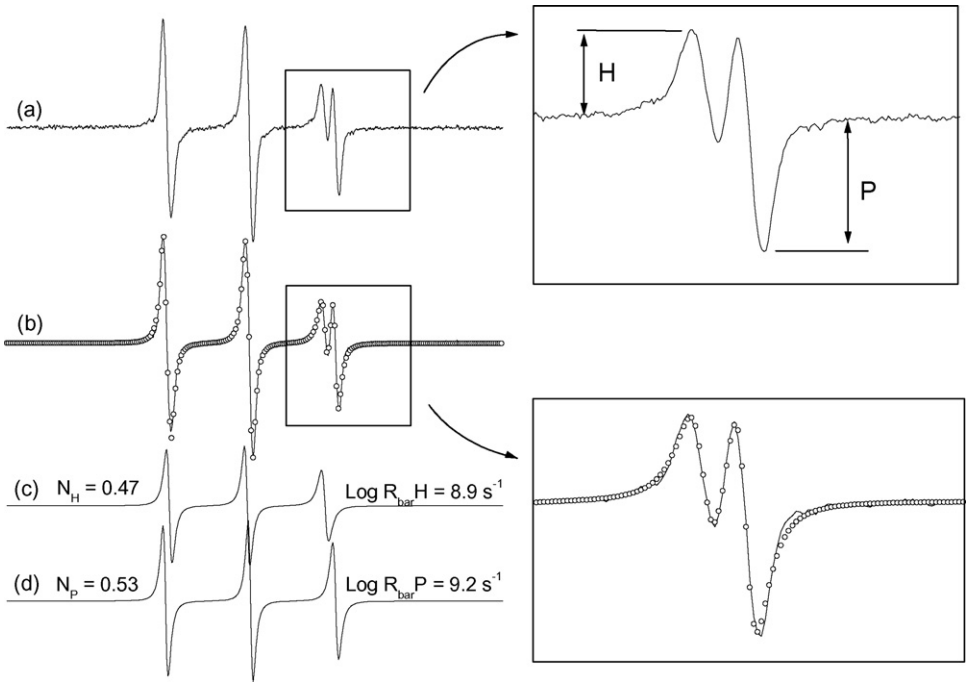

Fig. 2. (a) EPR spectrum of spin label TEMPO in stratum corneum (pH 5.5, 50 °C) and the spectral parameters H and P that define the parameter $f = H/(H + P)$. (b) The same spectrum (line) with its best-fit EPR spectrum (empty circles) superimposed. The best-fit spectra in this study were obtained by NLLS fits, using a simulation model of two spectral components. The component H (spectrum c) refers to the spin label fraction in the hydrophobic environment and the component P (spectrum d) is generated by the spin probes in the solvent. For clarity, the spectrum region in the box was magnified. The figure also indicates the fitting results: the percentage of spin label in each component, N_H and N_P, and their respective logarithm of average rotational diffusion constants, $\log R_{bar}H$ and $\log R_{bar}P$. The total scan range of the magnetic field was 65 G.

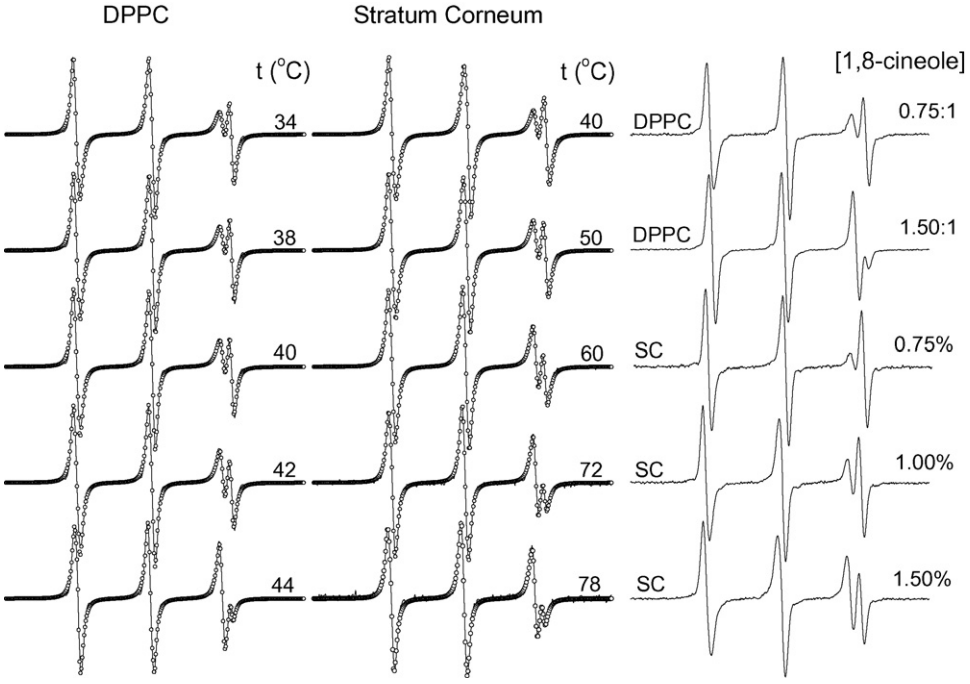

Fig. 3. Experimental (line) and best-fit (empty circles) EPR spectra of TEMPO in DPPC and stratum corneum (SC) membranes at several temperatures and concentrations of 1,8-cineole at 24 °C (given in a 1,8-cineole:DPPC molecular ratio or percentage of 1,8-cineole in SC). The total scan range of the magnetic field was 65 G.

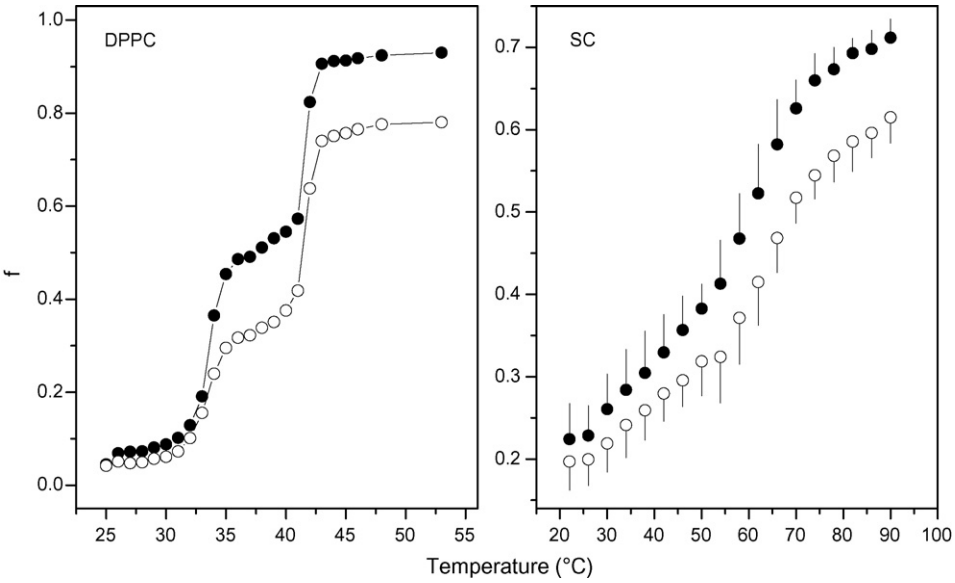

Fig. 4. Spectral parameter $f = H/(H + P)$ as described in Fig. 2 (solid circles) and relative population of TEMPO in component H (open circles) determined by spectral simulation for multilamellar vesicles of DPPC (left side) and stratum corneum (right side) membranes vs. temperature.

According to the solubility–diffusion mechanism, the permeability coefficient, P, of a molecule crossing a bilayer membrane is generally related to the partition coefficient in the bilayer, K, the diffusion constant across it, D, and the bilayer thickness, Δx, according to the following equation (Finkelstein, 1976):

$$P = \frac{KD}{\Delta x}. \tag{1}$$

The diffusion coefficient is defined as:

$$D = \frac{KT}{6\pi\eta r}, \tag{2}$$

where KT is the thermal energy, η the membrane viscosity and r is the molecular radius. The partition coefficient is the equilibrium ratio of the solute concentration in the bilayer, c_H, and in aqueous concentration, c_P. K can be determined if the relative volumes of membrane and solvent in the sample are known.

$$K = \frac{c_H}{c_P}, \tag{3}$$

or

$$K = \frac{N_H / V_{membrane}}{N_P / V_{solvent}}, \tag{4}$$

where N_H and N_P are the relative spin label populations in the hydrophobic and polar environments, respectively, which are provided by the fitting program. The relative membrane–solvent volumes for the two systems were estimated taking into account the sample volume within the capillary tube (about 15 μL) and the weights before and after drying the sample; the water content in the samples (w/w) was on average 65% for DPPC and 67% for SC. In the calculation of K, several assumptions were made: (a) in the case of SC, the membrane volume corresponds to 20% of the tissue, (b) the spin label is distributed throughout the membrane, (c) the relative volumes of solvent and membrane do not change in the measured temperature range and (d) it was estimated that the terpenes in the concentration used here increase the membrane volume by 15%.

The standard Gibbs free energy change required to transfer a molecule from an aqueous to a hydrocarbon phase, ΔG°, can be calculated based on the partition coefficient, as follows (Rogers and Wong, 1980; Da et al., 1992):

$$\Delta G^\circ = -RT \ln K, \tag{5}$$

or

$$\ln K = -\frac{\Delta H^\circ}{RT} + \frac{\Delta S^\circ}{R}, \tag{6}$$

where R is the gas constant, T the absolute temperature, ΔH° the standard enthalpy change for transferring the permeating molecules from solvent to the interior of the membrane and ΔS° is the associated entropy change. These thermodynamic parameters can be determined from the van't Hoff plots shown in Fig. 5. In this type of plot, the slope coefficient of each curve should give $\Delta H^\circ/R$ and the intercept should yield $\Delta S^\circ/R$. The calculated values of ΔG°, ΔH° and ΔS° for the control curves of DPPC and SC membranes are shown in Table 1. It is important

Table 1
Changes in standard Gibbs free energy (at 26 °C), enthalpy and entropy accompanying the transference of spin label TEMPO from the water to the DPPC or stratum corneum (SC) membranes

Samples	$\Delta G^\circ_{w\to m}$ (kcal mol^{-1})	$\Delta H^\circ_{w\to m}$ (kcal mol^{-1})	$\Delta S^\circ_{w\to m}$ (cal mol^{-1} K^{-1})
DPPC 35–41 °C	−0.4[a]	14.3	49.2
DPPC 43–53 °C	−1.9	6.5	28.2
SC 22–54 °C	−0.7	5.6	21.0
SC 54–70 °C	−0.1	12.4	41.8
SC 70–90 °C	−1.2	4.5	18.8

[a] The numerical values were calculated based on Eqs. (5) and (6), using the data from the van't Hoff graph (Fig. 5).

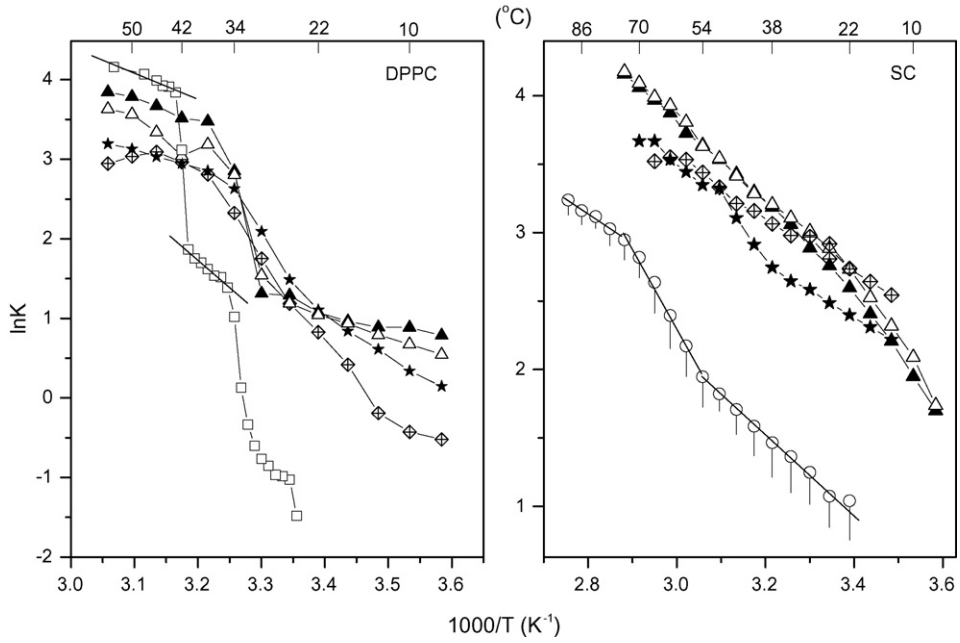

Fig. 5. Natural logarithm of partition coefficient *K* for DPPC (left side) and stratum corneum (right side) membranes vs. the reciprocal absolute temperature. Terpenes were added at a terpene:DPPC molar ratio of 0.75:1 or at 0.4% terpene in stratum corneum. Symbols: DPPC (control), open squares; stratum corneum (control), open circles; DL-menthol, solid triangles; α-terpineol, open triangles; 1,8-cineole, stars and (+)-limonene, diamonds.

to note that, to determine the parameter ΔH°, unlike ΔG° and ΔS°, it is not necessary to know the relative membrane–water volume in the sample, i.e., the calculation of the enthalpy change does not depend on the actual value of *K*; therefore, it is a more accurate determination.

In the presence of terpenes, the transition of DPPC at 42 °C appears between 32 and 38 °C and the gel phase seems to be transformed into the ripple phase. The DPPC membrane was more affected by terpenes in the temperature range corresponding to the gel phase (6–32 °C) and did not undergo alterations when in the liquid crystalline phase. In contrast, the SC samples presented increases of TEMPO partitioning caused by terpenes in the entire temperature interval measured. This was probably due to the fact that the DPPC bilayers in the liquid crystalline phase already reached the maximum disorder effect for the molecular ratio of terpene:DPPC (0.75:1) employed. The enthalpy and entropy changes observed in the presence of terpenes were essentially the same as those of the control samples (data not included in Table 1).

3.3. Molecular dynamics of TEMPO in the hydrocarbon phase

The logarithm of the average rotational diffusion constant of component *H*, $R_{bar}H$, plotted as a function of the reciprocal absolute temperature, is shown in Fig. 6. This Arrhenius plot allows us to calculate the apparent activation energy, E_a, of rotational motion in the regions of linear dependence, using the following equation:

$$\log R_{bar}H = A \exp\left(\frac{-E_a}{RT}\right), \quad (7)$$

where *A* is a pre-exponential factor. E_a is the energy barrier that the spin probe must overcome to achieve higher states of motion. Some E_a values obtained from this plot are presented in Table 2. It is interesting to note that the rotational diffusion rates of the spin probe also reflected the phase transitions of the membranes similarly to the partition coefficient (Fig. 5), and that, in the case of DPPC, the terpenes exerted similar effects on the two parameters. The terpenes did not increase the rotational motion of the spin probe in the fluid phase of DPPC bilayers, where it presented high partition coefficients. In the lower range of temperatures, the terpenes showed significant increases in probe dynamics in DPPC bilayers, while the SC treated with the terpenes DL-menthol and α-terpineol displayed a tendency to reduce the motion parameter to values considerably below the control. This fact is probably associated with the melting point of these terpenes, which ranges from 32 to 41 °C. It is worth mentioning that the comparative results between these terpenes were always very similar.

Fig. 7 shows the temperature dependence of the logarithm of $R_{bar}H$ and $R_{bar}P$ for the control samples of the two sys-

Table 2
Activation energy for the rotational diffusion of spin label TEMPO in DPPC or stratum corneum (SC) membranes

Samples	E_a (kcal mol^{-1})
DPPC 35–40 °C	8.7[a]
DPPC 43–53 °C	4.3
SC 22–54 °C	1.8
SC 54–70 °C	3.8
SC 70–90 °C	1.7

[a] The numerical values were calculated based on Eq. (7) and on data from the graph of Fig. 6.

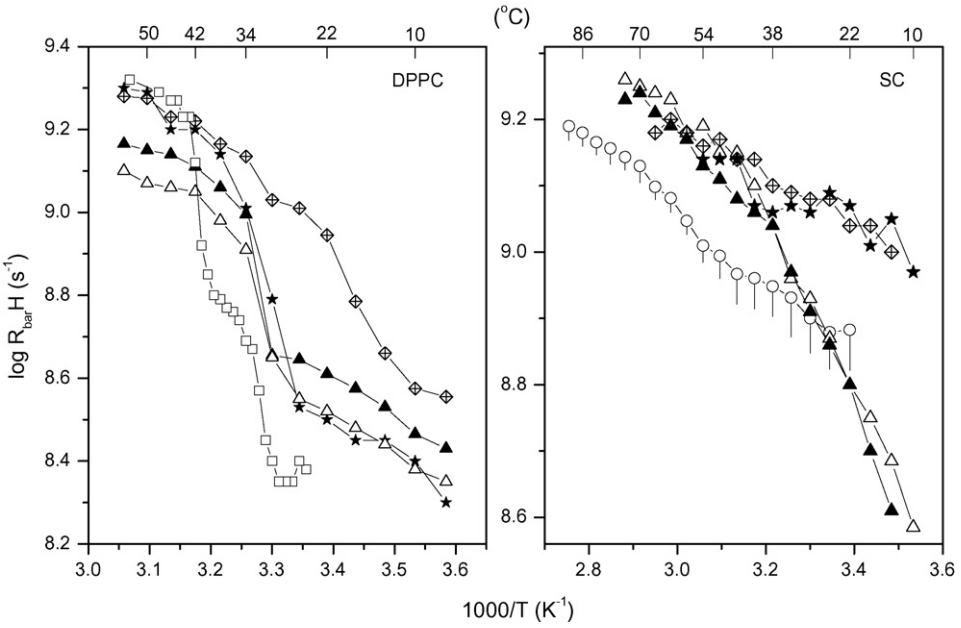

Fig. 6. Rotation diffusion rates (log $R_{bar}H$) for DPPC (left side) and stratum corneum (right side) membranes vs. the reciprocal absolute temperature. Terpenes were added at a terpene:DPPC molar ratio of 0.75:1 or at 0.4% terpene in stratum corneum. Symbols: DPPC (control), open squares; stratum corneum (control), open circles; DL-menthol, solid triangles; α-terpineol, open triangles; 1,8-cineole, stars and (+)-limonene, diamonds.

tems. Interestingly, the rotational motion of the spin probe in the polar environment decreased with the temperature and also reflected the phase transitions of DPPC bilayers. Furthermore, when these bilayers reached the fluid phase, the probe mobility was similar in both aqueous and hydrocarbon phases. In SC, this effect occurred at around 78 °C. This result suggests that the spin probes of the aqueous phase interact with the polar interface and that this interaction, which increases with temperature, is also modulated by the membrane phases.

To examine the location of TEMPO inside the bilayer and to determine if the terpenes can change this location, the hyperfine couplings constant, a_0, which is dependent on local environmental polarity, was measured in the two studied systems in the presence and absence of terpenes (Table 3). Measurements of the a_0 parameter have been reported for spin-labeled glycerophospholipids with the nitroxide group (doxyl) at position n in the *sn*-2 chain (n-PCSL) in DPPC membranes, whose values of 15.1 G for $n = 4$ and 14.5 G for $n = 16$ (Kurad et al., 2003) correspond to a decrease of 0.6 G along the lipid chain. Because the a_0 value observed for TEMPO in DPPC is 16.0 G (Table 3) and is therefore a higher value, it has often been inferred that the major probe location is near the polar interface. However,

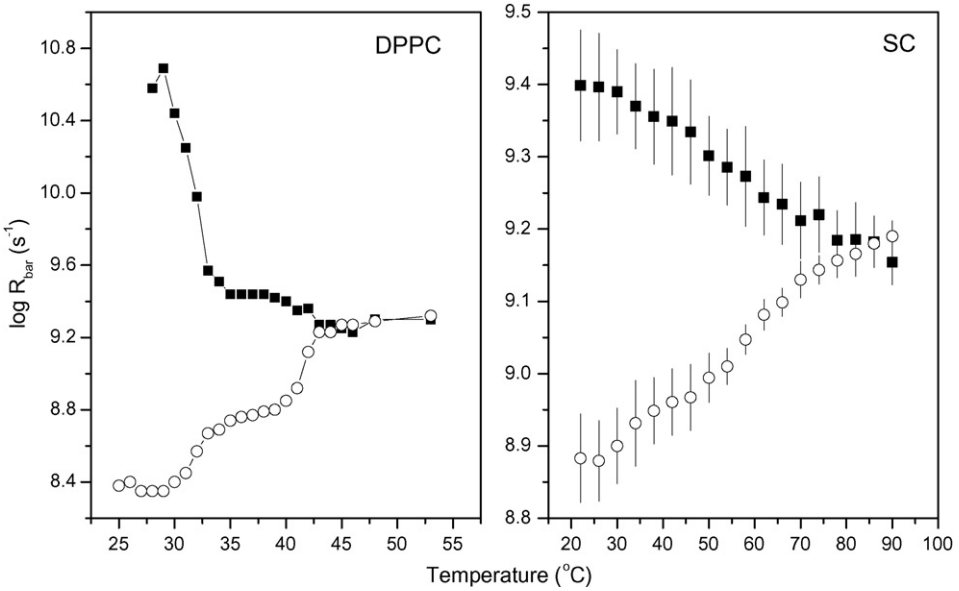

Fig. 7. Rotational diffusion rates, log $R_{bar}H$ (open circles) and log $R_{bar}P$ (solid squares), for DPPC (left side) and stratum corneum (right side) membranes vs. temperature.

Table 3
Isotropic ^{14}N-hyperfine splitting constant, a_0, at 25 °C

Samples	DPPC[a]	SC[b]	Terpene
Control	16.0[c]	16.0	–
1,8-Cineole	16.0	16.0	15.6
α-Terpineol	16.2	16.1	16.1
DL-Menthol	16.2	16.1	16.0
(+)-Limonene	16.1	15.9	15.7

This EPR parameter reflects the polarity within the membrane. In the aqueous phase a_0 was of 17.0 G.
[a] The terpene:DPPC molar ratio was 0.75:1.
[b] 0.5% terpene.
[c] The error associated with these experimental measurements is 0.1 G.

the measured a_0 parameter in (+)-limonene was 14.5 G for spin label 5-doxyl stearic acid and 15.7 G for TEMPO. Assuming that this difference of 1.2 G between these two spin labels also occurs in DPPC membranes, the corresponding values expected for TEMPO in DPPC bilayers would be around 16.3 G in the region close to the polar headgroups and 15.7 G in the central region of the bilayer. Thus, the a_0 value of 16.0 G observed for TEMPO in DPPC membrane coincides with the mean value of 15.7–16.3 G, and would be consistent with the nitroxide distributed throughout the membrane. Furthermore, since TEMPO is a small molecule of fast rotational motion, its stability in the headgroups region should be restricted and if located in a specific region of higher polarity in the membrane, it would be reasonable to expect relocations of the probe when increasing the temperature or in the presence of terpenes, thus reducing the a_0 value; however this alteration was not observed.

4. Discussion

The lipid composition of SC is unusual and its organization is quite complex. In human SC, nine subclasses of ceramides have been identified (Bouwstra and Ponec, 2006), together with long chain free fatty acids, cholesterol and cholesteryl sulfate, organized in crystalline lamellar phases. Small-angle X-ray diffraction studies on human, mouse and pig SC have shown that there are two lipid lamellar phases with repeated distances of ∼6 and 13 nm, which disappear between 60 and 75 °C (Bouwstra et al., 1991, 1992; White et al., 1988; Bouwstra and Ponec, 2006). Wide angle X-ray diffraction (Bouwstra et al., 1992; White et al., 1988) and electron diffraction techniques (Pilgram et al., 1999) have shown that the lateral lipid packing is orthorhombic at room temperatures, with a transition to a hexagonal lateral sublattice occurring between 30 and 40 °C (Pilgram et al., 1999; Bouwstra and Ponec, 2006). The hexagonal structure disappears between 75 and 95 °C (Bouwstra et al., 1992; White et al., 1988), with a probable change to a liquid crystalline phase. Although the lipids in the lamellar phases form predominantly crystalline lateral phases, a subpopulation of lipids probably coexists in the liquid phase (Bouwstra and Ponec, 2006).

Fourier-transformed infrared spectroscopy (FTIR) has been used to investigate thermotropic phase behaviors in porcine SC and its extracted lipids (Ongpipattanakul et al., 1994) and in model SC lipid mixtures (Narishetty and Panchagnula, 2005; Gooris and Bouwstra, 2007). The thermal behavior of the partitioning and rotational motion of TEMPO in SC membranes presented here is in close agreement with that of methylene stretching vibrations, which are directly related to the conformational order of lipid alkyl chains. For porcine SC, a more pronounced increase of νsCH_2 has been reported in the temperature range of 60–80 °C, which was associated with alkyl chain-melting (Ongpipattanakul et al., 1994). This lipid reorganization that occurs with a midpoint at around 70 °C is related with the disappearance of the lamellar structure and the probable phase transition hexagonal liquid packing observed by X-ray diffraction.

Comparing the thermotropic response of DPPC and SC membranes in Figs. 4 and 5, one can see several notable differences. DPPC is characterized by sharp increases in the partition coefficients and rotational diffusion rates following their two phase transitions at 34 and 42 °C, whereas the SC membrane presented slight increases in these two EPR parameters, even in the temperature interval of ∼54–70 °C where its main phase transition occurs, as characterized by X-ray diffraction and FTIR spectroscopy (Ongpipattanakul et al., 1994; Bouwstra and Ponec, 2006; Gooris and Bouwstra, 2007). In the temperature range of this phase transition in SC (∼54–70 °C), the ΔH° and ΔS° values are comparable to those observed for the ripple structure $P_{\beta'}$ of DPPC bilayer. Moreover, the activation energies associated with the rotational motion were consistently greater for DPPC (Table 2). While the rotational motion parameter of the probe, $\log R_{bar}$, varied from ∼8.4 to 9.3 s^{-1} for DPPC in a temperature interval of about 20 °C (∼30–50 °C), a smaller variation of ∼8.9–9.2 s^{-1} was observed for SC membranes in a wider temperature range of 22–90 °C, denoting that the membrane reorganizations induced by temperature are much greater in DPPC than in SC membrane. It is well known that phospholipid bilayers can exhibit dramatic increases in permeability to small water-soluble molecules in the regions of two-phase gel–liquid crystalline coexistence (Bramhall et al., 1987; Clerc and Thompson, 1995; Kraske and Mountcastle, 2001). This phenomenon can be attributed to an increase in permeability at the domain boundaries (Clerc and Thompson, 1995; Sparr and Wennerström, 2001), where two phases coexist at equilibrium. The suggested mechanisms for this high permeability have focused on density fluctuations in the boundary regions between the coexistent phases (Clerc and Thompson, 1995), which increase the probability of the formation of defects or transient holes that raise the bilayer's permeability to its maximum at T_m (Clerc and Thompson, 1995). In this context, the probability expected for defect formation in the SC membranes should be low in view of the results presented in this work, which indicate their high stabilities. Measurements of water permeability in porcine SC have revealed that the activation energy for water flux is 17.2 kcal mol^{-1} over a temperature range of 22–70 °C and 5.7 kcal mol^{-1} above 70 °C, indicating that the barrier function of SC is only reduced at high temperatures (Golden et al., 1987).

EPR experiments showed that terpenes at a terpene:DPPC molar ratio of 0.75:1 act to increase both the partition and rotational motion of the spin probe, except above 42 °C. In the

presence of terpenes, the transition of DPPC at ∼42 °C became less pronounced and declined to about 33 °C, while the transition at ∼34 °C did not occur (Figs. 5 and 6). The terpenes acted mainly in the gel phase, which appeared to have been transformed into the ripple structure. The plots in Figs. 5 and 6 do not show this transformation very clearly, since the terpenes altered the main phase transition of SC (∼60 °C). Because the curve of the partition coefficient in the case of 1,8-cineole seems to have a similar profile as that of the control, one can deduce that this transition temperature was reduced to around 45 °C. DSC experiments have identified four phase transitions in neonatal rat SC (used in this work) at about at 42 °C (T_1), 55 °C (T_x), 70 °C (T_2) and 78 °C (T_3), which has been attributed to lipid melting (Al-Saidan, 2004). The two major phase transitions in human SC occur at 72 °C (T_2) and 83 °C (T_3), and the terpenes D-limonene and 1,8-cineole have been found to reduce the temperatures of these two transitions by about 20 °C (Cornwell et al., 1996).

In this work, we studied two terpenes containing hydrogen-bonding donor groups (DL-menthol and α-terpineol), one with a hydrogen-bonding acceptor group (1,8-cineole) and one that does not form hydrogen bonds (hydrocarbon (+)-limonene). The parameters measured here showed similar results for these terpenes, and a discrepancy was only observed for the rotational motion parameter of DL-menthol and α-terpineol in SC, which showed a pronounced reduction of this parameter at temperatures below their melting point. Although terpenes can, in principle, weaken the hydrogen-bonding interactions at the membrane–water interface, these results suggest that the effects of terpenes on the membranes do not necessarily depend on direct competition for H-bonds with the polar headgroups.

In conclusion, the EPR spectroscopy of the spin label TEMPO provided new complementary information on the dynamics of SC lipids. Its partition coefficient between the aqueous and hydrocarbon phases as well as its rotational motion parameter reflected the phase transitions of the SC membranes, which are in agreement with data obtained by other techniques such as X-ray diffraction and FTIR. In the presence of 0.4% terpenes, both the probe partition and its dynamics in the bilayers were increased. The interaction of terpenes with the phospholipid bilayer was similar to that with the SC membranes in several aspects and indicated that the action of terpenes is stronger on ordered lipids. These results suggest that the effects of terpenes do not depend on specific characteristics of SC membranes and that the basic characteristics for terpenes to affect membranes are their ability to penetrate the bilayer, due to their highly hydrophobic character and their low molecular weight, around 150 g, leading to a distribution throughout the bilayer, especially at higher concentrations. On a scale of fast rotational motion, these molecules, acting effectively as spacers, destabilize the lipid tail packing and weaken the hydrogen-bonded network of the polar interface. This process may facilitate the partitioning of small polar molecules and, hence, their permeation through membranes.

Acknowledgements

This work was supported by CNPq (Conselho Nacional de Desenvolvimento Científico e Tecnológico) through a research grant (472273/03-5), a grant to A. Alonso (305900/2004-8) and a student fellowship to J.L.V. Anjos and by FUNAPE (Fundação de Apoio à Pesquisa—UFG).

References

Alonso, A., Meirelles, N.C., Tabak, M., 1995. Effect of hydration upon the fluidity of intercellular membranes of stratum corneum: an EPR study. Biochim. Biophys. Acta 1237, 6–15.

Alonso, A., Meirelles, N.C., Yushmanov, V.E., Tabak, M., 1996. Water increases the fluidity of intercellular membranes of stratum corneum: correlation with water permeability, elastic, and electrical properties. J. Invest. Dermatol. 106, 1058–1063.

Alonso, A., Meirelles, N.C., Tabak, M., 2000. Lipid chain dynamics in stratum corneum studied by spin label electron paramagnetic resonance. Chem. Phys. Lipids 104, 101–111.

Al-Saidan, S.M., 2004. Transdermal self-permeation enhancement of ibuprofen. J. Controlled Release 100, 199–209.

Anjos, J.L.V., Neto, D.S., Alonso, A., 2007. Effects of ethanol/L-menthol on the dynamics and partitioning of spin-labeled lipids in the stratum corneum. Eur. J. Pharmaceut. Biopharmaceut. 67, 406–412.

Anjos, J.L.V., Neto, D.S., Alonso, A., 2007a. Effects of 1,8-cineole on the dynamics of lipids and proteins of stratum corneum. Int. J. Pharm. 345, 81–87.

Barry, B.W., 1991. Lipid–protein-partitioning theory of skin penetration enhancement. J. Controlled Release 15, 237–248.

Bouwstra, J.A., Honeywell-Nguyen, P.L., 2002. Skin structure and mode of action of vesicles. Adv. Drug Deliv. Rev. 54, S41–S55.

Bouwstra, J.A., Ponec, M., 2006. The skin barrier in healthy and diseased state. Biochim. Biophys. Acta 1758, 2080–2095.

Bouwstra, J.A., Gooris, G.S., van der Spek, J.A., Bras, W., 1991. Structural investigations on human stratum corneum by small-angle X-ray scattering. J. Invest. Dermatol. 97, 1005–1012.

Bouwstra, J.A., Gooris, G.S., Salomons-de Vries, M.A., van der Spek, J.A., Bras, W., 1992. Structure of human stratum corneum as function of temperature and hydration: a wide angle X-ray diffraction study. Int. J. Pharm. 84, 205–216.

Bramhall, J., Hofmann, J., DeGuzman, R., Montestruque, S., Schell, R., 1987. Temperature dependence of membrane ion conductance analyzed by using the amphiphilic anion 5/6-carboxyfluorescein. Biochemistry 26, 6330–6340.

Budil, D.E., Lee, S., Saxena, S., Freed, J.H., 1996. Nonlinear-least-squares analysis of slow-motional EPR spectra in one and two dimensions using a modified Levenberg–Marquardt algorithm. J. Magn. Reson. A 120, 155–189.

Clerc, S.G., Thompson, T.E., 1995. Permeability of dimyristoyl phosphatidylcholine/dipalmitoyl phosphatidylcholine bilayer membranes with coexisting gel and liquid–crystalline phases. Biophys. J. 68, 2333–2341.

Cornwell, P.A., Barry, B.W., 1994. Sesquiterpene components of volatile oils as skin penetration enhancers for the hydrophilic permeant 5-fluorouracil. J. Pharm. Pharmacol. 46, 261–269.

Cornwell, P.A., Barry, B.W., Bouwstra, J.A., Gooris, G.S., 1996. Modes of action of terpene penetration enhancers in human skin; differential scanning calorimetry, small-angle X-ray diffraction and enhancer uptake studies. Int. J. Pharm. 127, 9–26.

Da, Y.-Z., Ito, K., Fujiwara, H., 1992. Energy aspects of oil/water partition leading to the novel hydrophobic parameters for the analysis of quantitative structure activity relationships. J. Med. Chem. 35, 3382–3387.

El-Kattan, A.F., Asbill, C.S., Michniak, B.B., 2000. The effect of terpene enhancer lipophilicity on the percutaneous permeation of hydrocortisone formulated in HPMC gel systems. Int. J. Pharm. 198, 179–189.

Finkelstein, A., 1976. Water and nonelectrolyte permeability of lipid bilayer membranes. J. Gen. Physiol. 68, 127–135.

Gao, S., Singh, J., 1998. In vitro percutaneous absorption enhancement of a lipophilic drug tamoxifen by terpenes. J. Controlled Release 51, 193–199.

Golden, G.M., Guzek, D.B., Kennedy, A.H., McKie, J.E., Potts, R.O., 1987. Stratum corneum lipid phase transitions and water barrier properties. Biochemistry 26, 2382–2388.

Gooris, G.S., Bouwstra, J.A., 2007. Infrared spectroscopic study of stratum corneum model membranes prepared from human ceramides, cholesterol, and fatty acids. Biophys. J. 92, 2785–2795.

Hori, M., Satoh, S., Maibach, H.I., Guy, R.H., 1991. Enhancement of propranolol hydrochloride and diazepam skin absorption in vitro: effect of enhancer lipophilicity. J. Pharm. Sci. 80, 32–35.

Jain, A.K., Thomas, N.S., Panchagnula, R., 2002. Transdermal drug delivery of imipramine hydrochloride. I. Effect of terpenes. J. Controlled Release 79, 93–101.

Kraske, W.V., Mountcastle, D.B., 2001. Effects of cholesterol and temperature on the permeability of dimyristoylphosphatidylcholine bilayers near the chain melting phase transition. Biochim. Biophys. Acta 1514, 159–164.

Kurad, D., Jeschke, G., Marsh, D., 2003. Lipid membrane polarity profiles by high-field EPR. Biophys. J. 85, 1025–1033.

Morimoto, H., Wada, Y., Seki, T., Sugibayashi, K., 2002. In vitro skin permeation of morphine hydrochloride during the finite application of penetration-enhancing system containing water, ethanol and L-menthol. Biol. Pharm. Bull. 25, 134–136.

Narishetty, S.T.K., Panchagnula, R., 2004. Transdermal delivery of zidovudine: effect of terpenes and their mechanism of action. J. Controlled Release 95, 367–379.

Narishetty, S.T.K., Panchagnula, R., 2005. Effect of L-menthol and 1,8-cineole on phase behavior and molecular organization of SC lipids and skin permeation of zidovudine. J. Controlled Release 102, 59–70.

Okabe, H., Takayama, K., Ogura, A., Nagai, T., 1989. Effect of limonene and related compounds on the percutaneous absorption of indomethacin. Drug Des. Deliv. 4, 313–321.

Ongpipattanakul, B., Francoeur, M.L., Potts, R.O., 1994. Polymorphism in stratum corneum lipids. Biochim. Biophys. Acta 1190, 115–122.

Pilgram, G.S.K., Pelt, A.M.E., Bouwstra, J.A., Koerten, H.K., 1999. Electron diffraction provides new information on human stratum corneum lipid organization studied in relation to depth and temperature. J. Invest. Dermatol. 113, 403–409.

Queirós, W.P., Neto, D.S., Alonso, A., 2005. Dynamics and partitioning of spin-labeled stearates into the lipid domain of stratum corneum. J. Controlled Release 106, 374–385.

Rogers, J.A., Wong, A., 1980. The temperature dependence and thermodynamics of partitioning of phenols in the *n*-octanol–water system. Int. J. Pharm. 6, 339–348.

Schneider, D.J., Freed, J.H., 1989. Spin labeling: theory and application. In: Berliner, L.J., Reuben, J. (Eds.), Biological Magnetic Resonance, vol. 8. Plenum Press, New York, pp. 1–76.

Shimshick, E.J., McConnell, H.M., 1973. Lateral phase separation in phospholipid membranes. Biochemistry 12, 2351–2360.

Smirnov, A., Smirnova, T., Morse, P.D., 1995. Very high frequency electron paramagnetic resonance of 2,2,6,6-tetramethyl-1-piperidinyloxy in 1,2-dipalmitoyl-*sn*-glycero-3-phosphatidylcholine liposomes: partitioning and molecular dynamics. Biophys. J. 68, 2350–2360.

Sparr, E., Wennerström, H., 2001. Responding phospholipid membranes—interplay between hydration and permeability. Biophys. J. 81, 1014–1028.

Vaddi, H.K., Ho, P.C., Chan, S.Y., 2002a. Terpenes in propylene glycol as skin-penetration enhancers: permeation and partition of haloperidol, Fourier transform infrared spectroscopy, and differential scanning calorimetry. J. Pharm. Sci. 91, 1639–1651.

Vaddi, H.K., Ho, P.C., Chan, Y.W., Chan, S.Y., 2002b. Terpenes in ethanol: haloperidol permeation and partition through human skin and stratum corneum changes. J. Controlled Release 81, 121–133.

Wang, D.-C., Taraschi, T.F., Rubin, E., Janes, N., 1993. Configuration entropy is the driving force of ethanol action on membrane architecture. Biochim. Biophys. Acta 1145, 141–148.

Wertz, P.W., Downing, D.T., 1987. Covalently bound ω-hydroxyacylsphingosine in the stratum corneum. Biochim. Biophys. Acta 917, 108–111.

White, S.H., Mirejovsky, D., King, G.I., 1988. Structure of lamellar lipid domains and corneocyte envelopes of murine stratum corneum. An X-ray diffraction study. Biochemistry 27, 3725–3732.

Williams, A.C., Barry, B.W., 2004. Penetration enhancers. Adv. Drug Deliv. Rev. 56, 603–618.

Yamane, M.A., Williams, A.C., Barry, B.W., 1995. Effects of terpenes and oleic acid as skin penetration enhancers towards 5-fluorouracil as assessed with time, permeation, partitioning and differential scanning calorimetry. Int. J. Pharm. 116, 237–251.